

Neutral Atomic Gas

Φ 29 Draine
Spitzer 3.35
3.42

(1)

Binney & Monfied 8.1A

1) Excitation of HI

Hyperfine $F=1-0$ spin-flip transition @ 21.105 cm
1420.406 MHz

with $g_z = 3$ ($2s+1$) and $g_1 = 1$ for stat. weights

$$\Delta E = h\nu = 5.9 \times 10^{-6} \text{ eV} = 0.069 \text{ K}$$

Level pops. determined by detailed balance

$$\gamma_{12} n_1 n_H + J_\nu B_{12} m_1 = \gamma_{21} n_2 n_H + J_\nu B_{21} m_2 + A_{21} n_2$$

$$\Rightarrow \frac{n_2}{n_1} = \frac{\gamma_{12}/\gamma_{21} + J_\nu B_{12}/\gamma_{21} n_H}{1 + (A_{21} + J_\nu B_{21})/\gamma_{21} n_H}$$

$$\text{Einstein relations} \Rightarrow A_{21} = \frac{2h\nu^3}{c^2} B_{21}, B_{21} = \frac{g_1}{g_2} B_{12}$$

$$\text{Boltzmann} \Rightarrow \gamma_{12} = \frac{g_2}{g_1} \gamma_{21} e^{-h\nu/kT_K} \leftarrow \text{kin. Temp.}$$

$$J_\nu \triangleq \frac{2\nu^2 k T_R}{c^2} \leftarrow \text{rad. Temp.} \quad (\text{i.e., BB with } \frac{h\nu}{kT_R} \ll 1)$$

$$\Rightarrow \frac{n_2}{n_1} = \frac{\frac{g_2}{g_1} \left[e^{-h\nu/kT_K} + (A_{21}/\gamma_{21} n_H) \frac{kT_R}{h\nu} \right]}{1 + (A_{21}/\gamma_{21} n_H) \left(1 + \frac{kT_R}{h\nu} \right)}$$

Since $kT_R/h\nu \gg 1$ for $T_c \geq 2.73 \text{ K}$, and $h\nu/kT_K \ll 1 \Rightarrow$

$$\frac{n_2}{n_1} \approx \frac{g_2}{g_1} \approx \frac{3}{1} \Rightarrow \boxed{\frac{n_2}{n_H} \approx \frac{3}{4}}$$

2) Radiation Transfer

$$\frac{dI_0}{ds} = \frac{\hbar\nu}{4\pi} \left[\underbrace{m_2 A_{21}}_{j\nu} - \underbrace{(m_1 B_{12} - m_2 B_{21})}_{K\nu} S_\nu \right]$$

$$S_\nu = \frac{j\nu}{K\nu} = \frac{m_2 A_{21}}{m_1 B_{12} - m_2 B_{21}}, \quad \text{source function}$$

$$\Rightarrow S_\nu = \frac{2h\nu^3/c^2 B_{21} m_2}{\left(\frac{g_2}{g_1} \frac{m_1}{m_2} - 1 \right) B_{21} m_2} = \frac{2h\nu^3/c^2}{\frac{g_2}{g_1} \frac{m_1}{m_2} - 1}$$

Using Einstein
relation, m_1)

$$\Rightarrow S_\nu = \frac{2h\nu^3}{c^2} \cdot \left[\frac{1}{1 + \left(A_{21}/\gamma_{21} m_H \right) \left(1 + \frac{KTR}{h\nu} \right)} - 1 \right] \\ = \frac{2h\nu^3}{c^2} \cdot \left[\frac{e^{-h\nu/kT_K}}{e^{-h\nu/kT_K} + \left(A_{21}/\gamma_{21} m_H \right) \left(\frac{KTR}{h\nu} \right)} \right]$$

$$\Rightarrow S_\nu = \frac{2h\nu^3}{c^2} \frac{kT_K}{h\nu} \left[\frac{e^{-h\nu/kT_K} + \frac{A_{21}}{\gamma_{21} m_H} \cdot \frac{KTR}{h\nu}}{1 + \frac{A_{21}}{\gamma_{21} m_H} \cdot \frac{KTR}{h\nu}} \right]$$

(3)

$[] \rightarrow \chi'$ of Sp.Tzer 4-15

$$[] \sim 1 - \frac{1}{23 n_H} \quad \text{for } T_K = 80K$$

$$A_{21} = 2.87 \times 10^{-15} s^{-1}, \quad \gamma_{21} \sim \text{few} \times 10^{-11} cm^3 s^{-1}$$

(8 $\times 10^{-11}$ for 80K) Sp.Tzer Table 4.2

$$\Rightarrow F_\nu \frac{T_K(K)}{n_H(cm^{-3})} \leq 10^2, \quad \frac{A_{21}}{\gamma_{21} n_H} \frac{k T_K}{h\nu} \ll 1$$

$$\text{if } T_R < T_K \Rightarrow \frac{A_{21}}{\gamma_{21} n_H} \frac{k T_R}{h\nu} \ll 1 \text{ also}$$

$$e^{-h\nu/kT_K} \approx 1 \Rightarrow \boxed{S_\nu \approx \frac{2 \nu^2 k T_K}{c^2}}$$

$$\text{More generally, define } S_P \triangleq \frac{2 \nu^2 k T_S}{c^2}, \quad T_S = \text{spin Temperature} \\ = T_K \cdot []$$

Spin Temp. is generally below T_K if gas is low density
since then $[]$ gets smaller.

$$\text{Optical depth: } d\tau_\nu = \frac{h\nu}{4\pi} (\mu_1 B_{12} - \mu_2 B_{21}) ds$$

For uniform medium, The solution of xfer. equation is:

$$I_\nu = I_\nu(0) e^{-\tau_\nu} + (1 - e^{-\tau_\nu}) S_\nu$$

Define brightness Temperature such that:

$$I_\nu \triangleq \frac{2 \nu^2 k T_B}{c^2}$$

(4)

\Rightarrow Solution is

$$T_B = T_B(0) e^{-\tau_v} + (1 - e^{-\tau_v}) T_s$$

Optically thin emission:

$$1 - e^{-\tau_v} = \tau_v \Rightarrow \Delta T_B \triangleq T_B - T_B(0) = (1 - e^{-\tau_v})(T_s - T_B(0)) = \tau_v (T_s - T_B(0))$$

$$\Rightarrow T_B \approx T_s \cdot \tau_v \text{ for small } T_B(0)$$

Absorption: $T_B(0) \gg T_s$

$$T_B(\text{ON}) - T_B(0) = \Delta T_B(\text{ON}) = T_B(0) (e^{-\tau_v} - 1) + T_s (1 - e^{-\tau_v})$$

$$T_B(\text{OFF}) - T_B(0) = \Delta T_B(\text{OFF}) = (1 - e^{-\tau_v}) T_s$$

$$\Rightarrow \Delta T_B(\text{ON}) - \Delta T_B(\text{OFF}) = T_B(0) (e^{-\tau_v} - 1)$$

$$\Rightarrow e^{-\tau_v} = 1 + \frac{\Delta T_B(\text{ON}) - \Delta T_B(\text{OFF})}{T_B(0)}$$

T_B away from line $\approx T_B(0)$

$\Rightarrow T_s, \tau_v$ are both determined

Optical depth and column:

$$\tau_v = \frac{h\nu}{4\pi} (\mu_1 B_{12} - \mu_2 B_{21}) s = \frac{h\nu}{4\pi} \underbrace{(\mu_1 B_{12} - \mu_2 B_{21})}_{\mu_2 A_{21}} s$$

$$= \frac{h\nu}{4\pi} \frac{1}{s_v} \cdot \mu_2 A_{21} s = \frac{h\nu}{4\pi} \frac{c^2}{2v^2 K T_s} \cdot \mu_2 \frac{2h\nu^3}{c^2} B_{21} s$$

$$= \left(\frac{h\nu}{4\pi}\right)^2 \frac{\mu_2 B_{21}}{K T_s} s \quad \text{and} \quad \mu_2 = \frac{g_2}{g_1} \mu_1, \quad B_{21} = \frac{g_1}{g_2} B_{12} \Rightarrow \mu_2 B_{21} = \mu_1 B_{12}$$

$$\Rightarrow T_D = (\nu \omega)^2 \cdot \frac{m_B \beta_{12}}{4\pi k T_S} s \quad , \quad \text{Birney + Men. field 8.18}$$

$$T_D = \frac{\nu \omega}{4\pi} \frac{c^2}{2\nu k T_S} A_{21} \cdot \frac{3}{4} \underbrace{\frac{m_B s}{\pi}}_{N_H} \Rightarrow \boxed{T_D = \frac{3}{32} \frac{h c^2 A_{21}}{v k T_S} N_H(v)}$$

$$N_H(v) dv = N_H(v) dv$$

$$\frac{dv}{v} = \frac{dv}{c} \Rightarrow dv = \frac{v}{c} dv = \frac{dv}{\lambda}$$

$$N_H(v) dv = N_{H,TOT} \cdot f(v) dv = N_{H,TOT} \cdot f(v) \lambda dv$$

$$= c \cdot \left(1 - \frac{v}{v_c}\right)$$

$$\Rightarrow N_H(v) = N_{H,TOT} \cdot f(v) \cdot \lambda$$

$$T_D = \underbrace{\frac{3 h c^2 \lambda}{32 \pi v k} A_{21}}_{\frac{3 h c \lambda^2 A_{21}}{32 \pi k}} \cdot \frac{N_{H,TOT} f(v)}{T_S}$$

$$T_D = \left(5.489 \times 10^{-14} \text{ K cm}^3 \text{s}^{-1} \right) \cdot \underbrace{\frac{N_{H,TOT} f(v)}{T_S}}_{\left(\frac{N_H}{\text{cm}^{-2}} \right) \cdot \left(\frac{f(v)}{\text{km s}^{-1}} \right) \left(\frac{1}{T_S / \text{K}} \right)}$$

Spitzer 3-37

$$\text{Since, for emission } T_D = \frac{T_B}{T_S} \quad (T_B(0) \text{ negligible})$$

$$\Rightarrow N_{H,TOT} = \frac{\int T_B(v) dv}{5.489 \times 10^{-14} \text{ K cm}^3 \text{s}^{-1}}$$

$$\Rightarrow \boxed{N_{H,TOT} = 1.82 \times 10^{18} \text{ cm}^{-2} \text{ K}^{-1} (\text{km s}^{-1})^{-1} \int T_B(v) dv} \quad \text{Spitzer 3-38}$$

(6)

Absorption-emission experiments can be used to determine both T and $T_B \Rightarrow$ yield $N_{H,TOT}$ and T_S

Typical lines of sight have a mix of warm and cold

Emission $\propto \int T_B d\sigma \Rightarrow$ yields Total column assuming $T < 1$, since upper level is always 3/4 of pop. no matter what.

$$T \propto \frac{N}{T_S} \Rightarrow T_{mix} \propto \frac{N_c}{T_c} + \frac{N_w}{T_w}$$

\Rightarrow because cold clouds have larger T in general, T_S tends to be dominated by their temperature.

Distribution Kulkarni & Heiles 1987

Wolfire et al 2003, ApJ 587, 278

@ solar neighborhood, looking \perp to the ~~galactic~~ Galactic plane,
 $\sum \sim 6.5 M_{\odot} pc^{-2}$ (Redba Krishnan et al, 1972)

CNM + WNM (HI emission) $\sum \sim 8 M_{\odot} pc^{-2}$ (Dickey + Lockman 1990)
 w/M $\sum \sim 2 M_{\odot} pc^{-2}$ (Reynolds)

CNM $\rightarrow 40\%$
 WNM $\rightarrow 60\%$
 (Heiles & Troland 2003)

Molec. $\sum \sim 1-2 M_{\odot} pc^{-2}$

\Rightarrow Total $\sum \sim 11-12 M_{\odot} pc^{-2}$

Melotte (1895), $H = 120 pc$ inside $R < 5 Kpc$

$H = 260 pc$ at Solar circle

Thickness (Lockman)

Possible mult. pl. comps. w/different thickness
 Average midplane density $M_{HI} = 0.6 cm^{-3}$ for $R = 4-12 Kpc$

CNM clouds, Temp + colum.

(Heiles + Troland 2003,
 ApJ 586, 1067)

Broad ($\gtrsim 9 km/s$) emission seen on all los at intermediate + high los. \rightarrow diffuse WNM

Narrow ($< 5 km/s$) seen in 1/3 \rightarrow CNM

(7)

\wedge → emission
 \vee → only narrow seen in absorption, why? "longer"

$\tau \propto \frac{1}{T_s}$ → narrow features are cold clouds
 broad features WNM

⇒ Doing emission-absorption studies yield $T_s \sim 50-200\text{K}$

$$N_H \sim 0.3 - 2 \times 10^{20} \text{ cm}^{-2}$$

"Median" cloud has $N_H = 0.8 \times 10^{20} \text{ cm}^{-2}$ at $T = 115\text{K}$, $\underline{T_{\text{peak}}} = 0.11$

Recent Heiles + Tielens:

mission	cold cloud	2×10^{20}	0.5×10^{20}
	warm cloud	8×10^{20}	1.3×10^{20}
$N_H = 10^{20} \text{ cm}^{-2} \Rightarrow \sum 1 \text{ Mpc}^3$	(b) < 10	$ b > 10$	

See Heiles & Tielens (2003) plots

Temperature of WNM

Requires OPT, IR, UV lines (HI obs are biased toward the cold)

Use HI emission to find components w/ absorption counterpart

Then linewidths give upper limits to Temperature.

$\sim \frac{1}{2}$ comps. have $T_E < 5000\text{K}$ (Heiles 2003)

Using optical + UV lines toward distant stars comb. with HI
 \downarrow \downarrow
 Ca Si, C, N, Mg, S space based

date, Fitzpatrick + Spitzer (1997) comp. Temperatures (+ ioniz. and density info) → Temp. upper limits of $5000-7000\text{K}$, but also some lower

Temp. ranges $\ll 8,000\text{K}$ for WNM are unstable if $P = \text{fixed}$)

but WNM has long cooling time

Density

From modeling opt/UV lines (Fitzpatrick + Spitzer)

n_e as small as 0.02 cm^{-3} near $\text{few} \times 0.01 - 0.1 \text{ cm}^{-3}$

If X_e known (or estimated) $\Rightarrow n = \frac{n_e}{X_e}$

X_e ?

E.g., assume single component, $X_e = \frac{n_{e\perp}}{n_{\text{WNM}}}$ from DM

Heiles (2000) local ISM $X_e = \frac{n_{e\perp}}{n_{\text{WNM}}} \sim 0.2$ from HI em.

$$X_e = \frac{n_{e\perp}}{n_{\text{WNM}}} \sim 0.2$$

$\Rightarrow n_{\text{WNM}} \sim \text{a few tens}$, but very uncertain.

CNM density? No direct probe.

Can assume pressure to derive: $n k T = P$, $n_{\text{typ}} \sim 100 \text{ cm}^{-3}$

If single spherical cloud observed, $\Rightarrow n$ from $\frac{N_{\text{HI}}}{L_{\text{size}}}$ for HI em.

\Rightarrow but probably clouds are sheets/flows and this is not a valid assumption

Heating-Cooling

Spitzer 5.1d, Wolfe et al. (1985), Wolfe et al. (2003)

Ionization \rightarrow 1) Cosmic rays



Coupled gas to "red" field

Primary CRs + secondary e^-

Primary e^- energy $\sim 35 \text{ eV}$

Volume CR ionization rate $\sim 3 \times 10^{-17} \text{ m cm}^{-3} \text{ s}^{-1}$

including (50%) effect of secondaries

(Solar wind screens low E_{CR})

3

2) Soft X-rays

Directly write H and He, primary e can ionize other elements

Rate ~~loss~~ depends on N_{H} To & X-ray source

$$\gamma \sim 10^{-15} \text{ s}^{-1} \text{ H}^{-1} \text{ To } 10^{-18} \text{ s}^{-1} \text{ H}^{-1} \text{ for } N = 10^{18} \text{ to } 10^{20} \text{ cm}^{-2}$$

Wolfe et al (1995)

Equil. ionization fraction is determined by balancing recomb. $\propto n_{\text{e}}^2$ with ioniz. rate.

Heating

CI: diffuse UV ionizes low-ion pot. atoms, particularly

Carbon

CI ion. is 11.3 eV

H ion is 13.6 eV \rightarrow so plenty of photons available

$$\frac{n_e}{n_H} \gg \frac{m_e}{m_H} = 4 \times 10^{-4} \times \frac{1}{d_C} \rightarrow \text{abundant}$$

\uparrow
gas phase depletion

FUV rad. field: Hobbing field (1968)

\uparrow
sufficient to
fully ionize CI

$$G_0 = 1.6 \times 10^3 \text{ erg cm}^{-2} \text{ s}^{-1}$$

More recent revisions (Draine, etc)

$$\chi = 1.7 G_0$$

Heating rate is ioniz. rate \times excess energy/ioniz.
 $\sim 2 \text{ eV}$

$$\text{ion rate} \equiv \text{recomb rate} = \alpha^{(2)} n_e^2$$

$$\Rightarrow \text{Heating rate is } \bar{E}_2 \alpha^{(2)} n_e^2 = \Gamma_c \cdot M$$

$$\text{CR : } \Gamma_{\text{CR}} \sim \bar{E}_2 \quad \bar{E} \sim 35 \text{ eV} \Rightarrow \Gamma_{\text{CR}} \sim 10^{-28} - 10^{-27} \text{ s}^{-1} \text{ H}^{-1}$$

$$\text{X-ray : Attenuation-dependent, } \Gamma_{\text{x-ray}} \sim 1 - \text{few} \times 10^{-27} \text{ erg s}^{-1} \text{ H}^{-1}$$

Photoelectric Heating

Gain are small, $\lambda = 3-100\text{\AA}$ $\gamma_{\text{obs. efficiency}} \sim 1$

Heating rate: $n\Gamma = n_d G_d \frac{4\pi J_p}{h\nu} \cdot Q \cdot \eta \cdot (\text{E - ion. pot.})$

Factors:
 \uparrow # density of grains
 \uparrow # of photons "quantum yield" ~ 0.1 for small grains + UV rad.
 \uparrow cross section (cm²)

$n\Gamma = 10^{-24} n \in G \text{ erg cm}^{-3} \text{ s}^{-1}$

\uparrow seed field in units of "Hobangs" ($1.6 \times 10^{-3} \text{ erg cm}^{-2} \text{ s}^{-1}$)
 fraction of UV obs by grains converted to gas heating

$$\epsilon = \frac{4.8 \times 10^{-2}}{1 + \left[\frac{(G T^{1/2})}{m_e} \right] / 1925}^{0.73} + \frac{3.7 \times 10^{-2} (T/10^4)^{0.7}}{1 + \left[\frac{(G T^{1/2})}{m_e} \right] / 5000}$$

\uparrow
Low T dominant

\uparrow
longer records. note at light
lower grain charge $\Rightarrow e$ more easily ejected.

Low $\frac{G T^{1/2}}{m_e} \rightarrow$ grains are neutral or negative, $\epsilon \sim 0.05-0.09$

high $\frac{G T^{1/2}}{m_e} \rightarrow$ pos. charge, ϵ lower

This is the dominant heating except @ very large density (CI heating \uparrow)

Cooling (@ Spitzer 6.2a)

$\text{Ly}\alpha$: @ high T e collisions excite H to $n=2$, radiating Ly α
 which is absorbed by dust ~~and~~ and radiated in IR

$$\Lambda = 7.3 \times 10^{-19} n_e n(H_2) e^{-1.2 \times 10^5/T} \text{ erg cm}^{-3} \text{ s}^{-1}$$

6-12 Spitzer

CII : CII fine structure line ($E = 0.0078 \text{ eV}$) @ $157.7 \mu\text{m}$
is collisionally excited and radiatively de-excited

Biggest cooling line in galaxies

$$\Lambda = 7.9 \times 10^{-27} n_{\text{H}}^2 \text{ cm}^{-3} \text{ s}^{-1} \text{ erg cm}^{-3} \text{ s}^{-1}$$

↑
depletion

SP-TZC 6-13

Other fine structure : OI ($63 \mu\text{m}$), CI ($608 \mu\text{m}, 370 \mu\text{m}$) may
be important depending on situation

Recomb. onto small grains : @ $T > 10^4 \text{ K}$ (low densities)

Thermal energy is lost by recomb. onto
 $\sim kT$
grains

$$n^2 \Lambda = 4.65 \times 10^{-30} T^{0.94} (G_e T^{1/2} / m_e)^\beta \text{ cm}^{-3} \text{ erg s}^{-1} \text{ cm}^{-3}$$

Wolfe
eq. 8

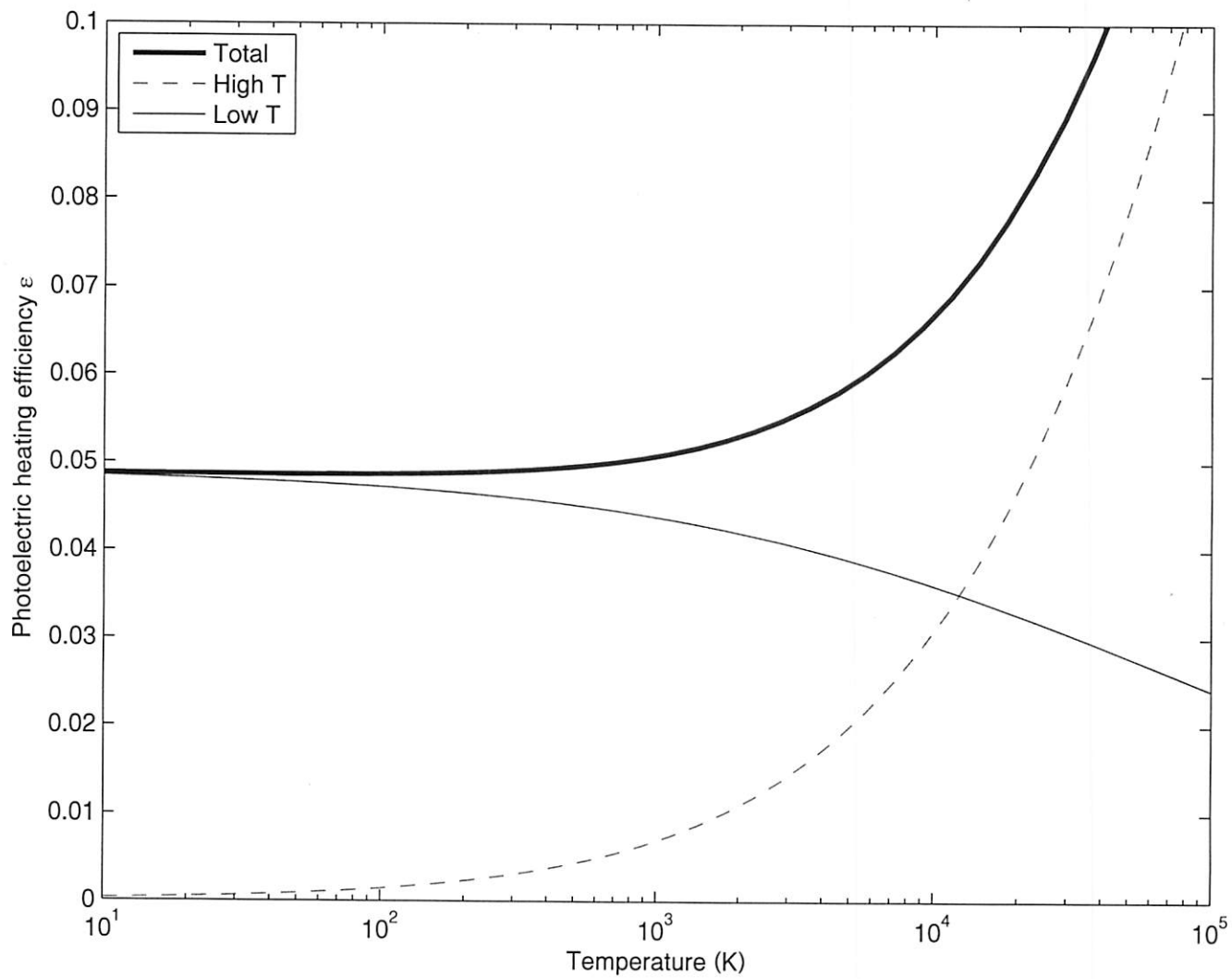
$$\beta = 0.74 / T^{0.68}$$

High density : PE heating and CII cooling dominate

Low dens : ~~PE~~ PE heating + Ly α + PE cooling

⇒ For fixed T , this indicates the stable equilibrium of
Two phases. We'll see this later

assuming $n_e = 0.1 \text{ cm}^{-3}$
 $G = 1$



experiments. Both may be the result of the passage of a shock front through a much larger cloud. The recently discovered structure in the ionized medium on scales of ~ 10 AU (92c, 281a) might be related to the small-scale structure in the cool neutral medium if, for example, both are caused by instabilities behind supernova shocks, but this connection is only speculative.

2.1.4 OBSERVING SELF-ABSORPTION Just as interstellar $\text{Ly}\alpha$ absorption can be detected against the broad $\text{Ly}\alpha$ emission lines from late-type stars, so too can a cold H I cloud appear in absorption against H I emission from warmer gas behind it. Two circumstances are illustrated in Figure 1, along with the 21-cm profiles that result: The telescope on the left measures the sum of the two profiles because the hot cloud is optically thin, and the telescope on the right sees a self-absorbed profile.

Self-absorption was first detected against the low-latitude, bright H I toward the galactic center and anticenter (109, 205). Its occurrence is direct evidence that the kinetic temperature of galactic H I has a large range.

The phenomenon can be difficult to recognize in a complex spectrum, and Knapp (144) has proposed that self-absorbed features be identified by

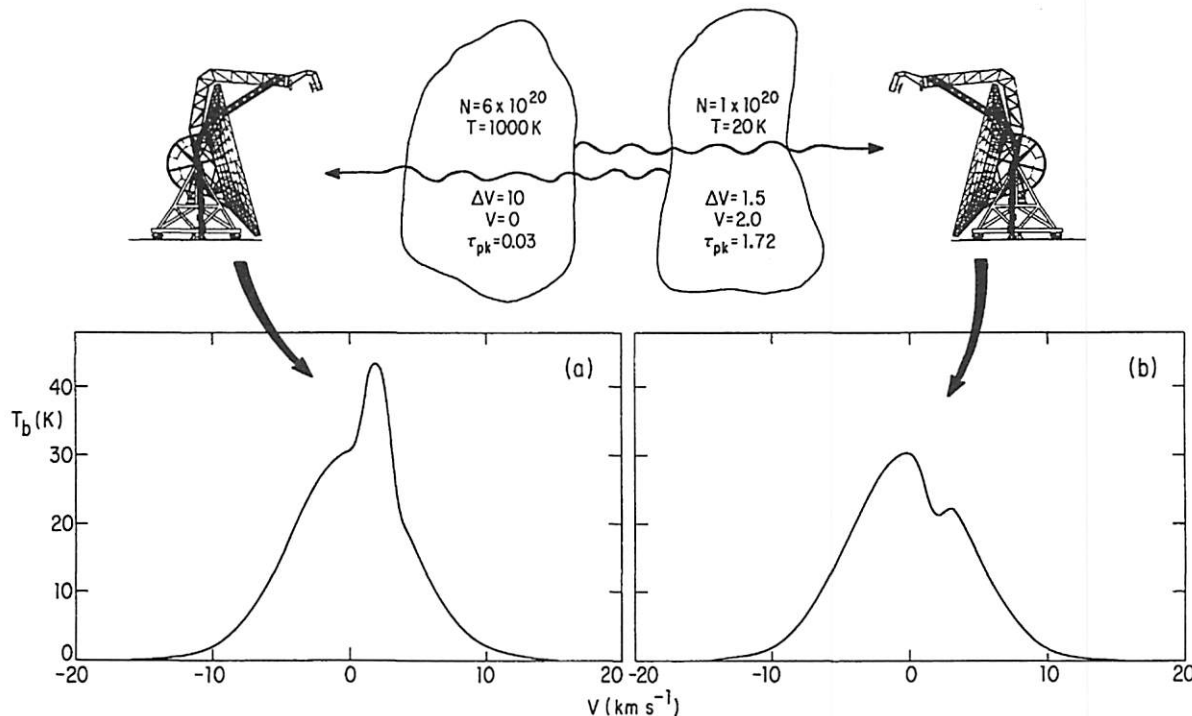
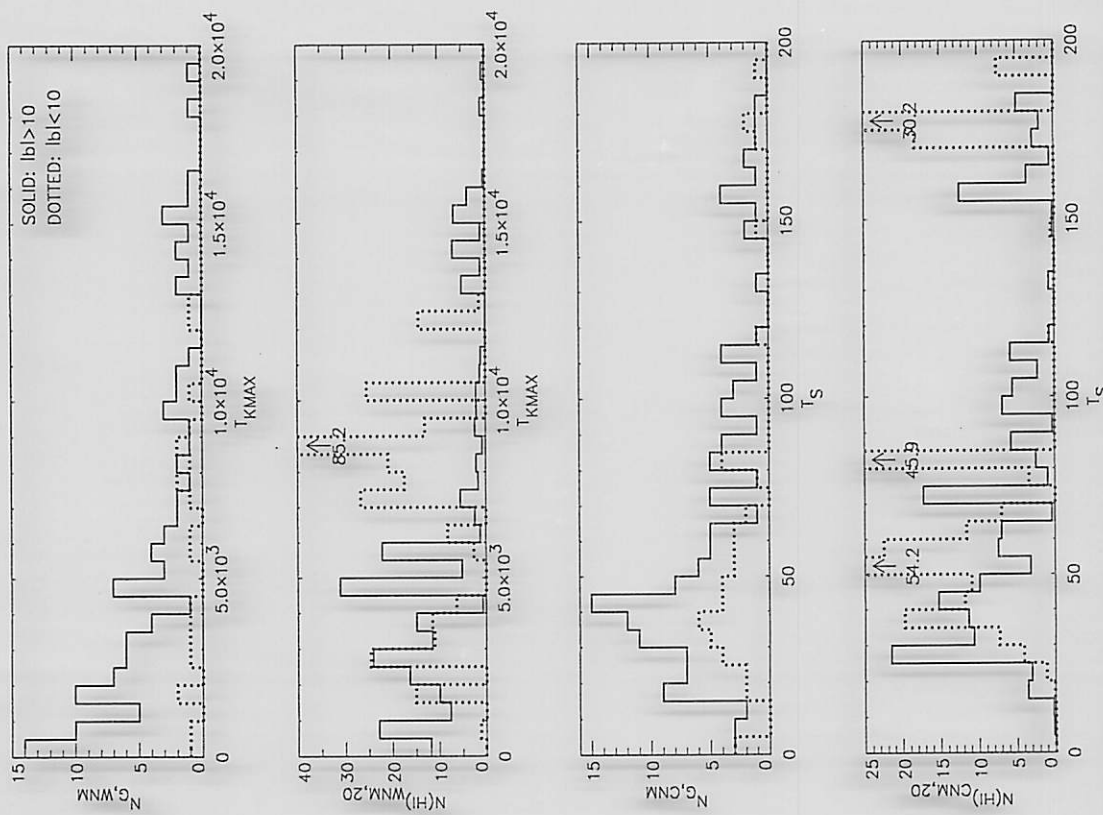


Figure 1 Schematic of the geometry of 21-cm self-absorption. The structure of an emission profile depends on the relative location of hot and cold clouds as viewed by the observer. Superpositions like this are very common at low and intermediate latitudes. The profile on the right (*b*) is self-absorbed.

Heiles & Trolend 2003

FIG. 2.—Histograms of $T_{k,\max}$ for the WNM (top two panels) and of T_s for the CNM (bottom two panels). The solid lines are for $|b| > 10^\circ$ and the dotted ones for $|b| < 10^\circ$. N_G is the number of Gaussian components; $N(\text{H I})_{20}$ is column density in units of 10^{20} cm^{-2} .



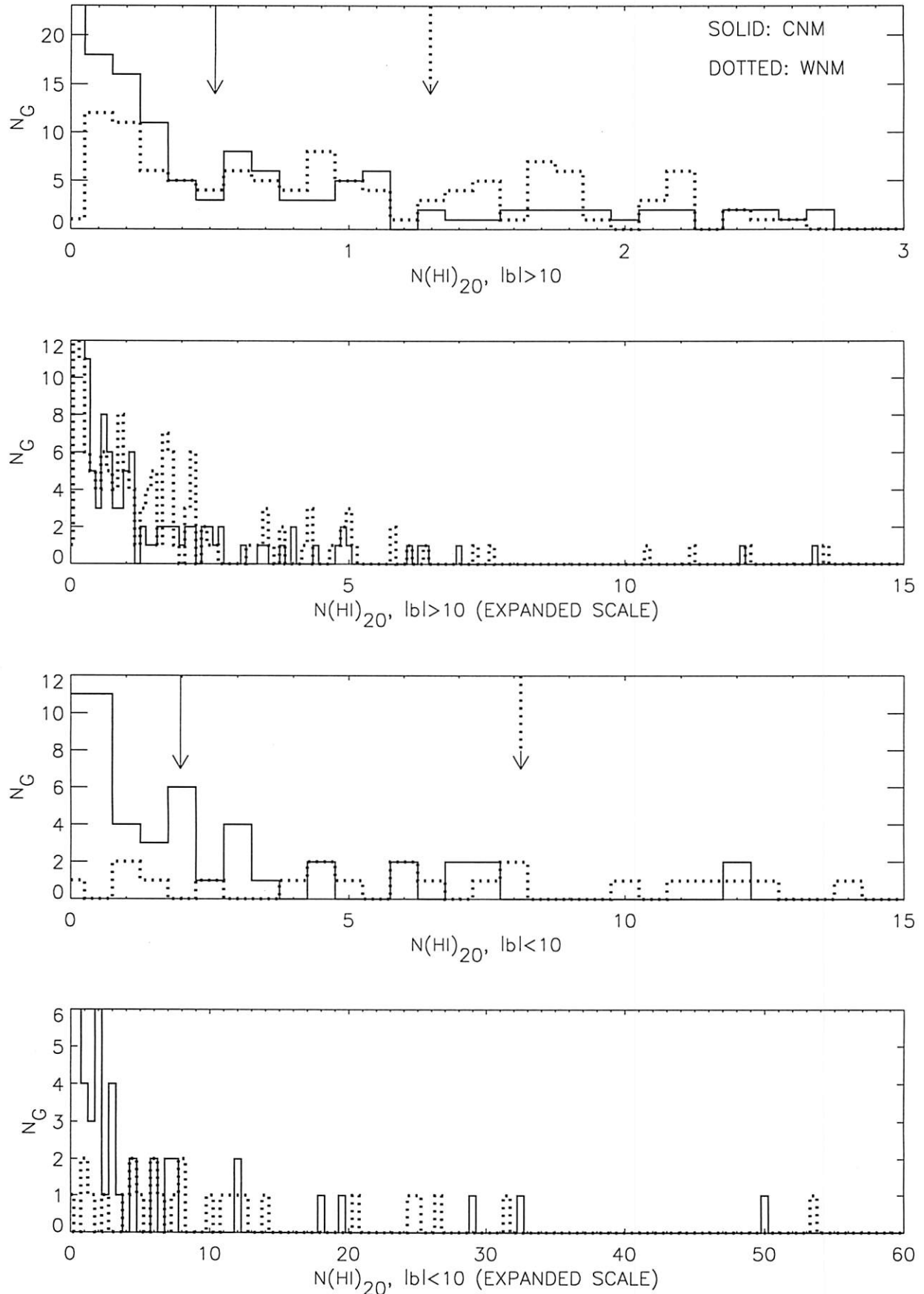


FIG. 4.—Histograms of number of Gaussians N_G and column densities $N(\text{H I})_{20}$ for all Gaussian components, both CNM (solid histogram) and WNM (dotted histogram). The top two panels show $|b| > 10^\circ$ with different scales on both axes to facilitate interpretation; the bottom two panels are for $|b| < 10^\circ$. The arrows show the medians, which are for the (CNM, WNM) of (0.60, 1.30) at $|b| > 10^\circ$ and (2.0, 5.0) at $|b| < 10^\circ$. $N(\text{H I})_{20}$ is in units of 10^{20} cm^{-2} .

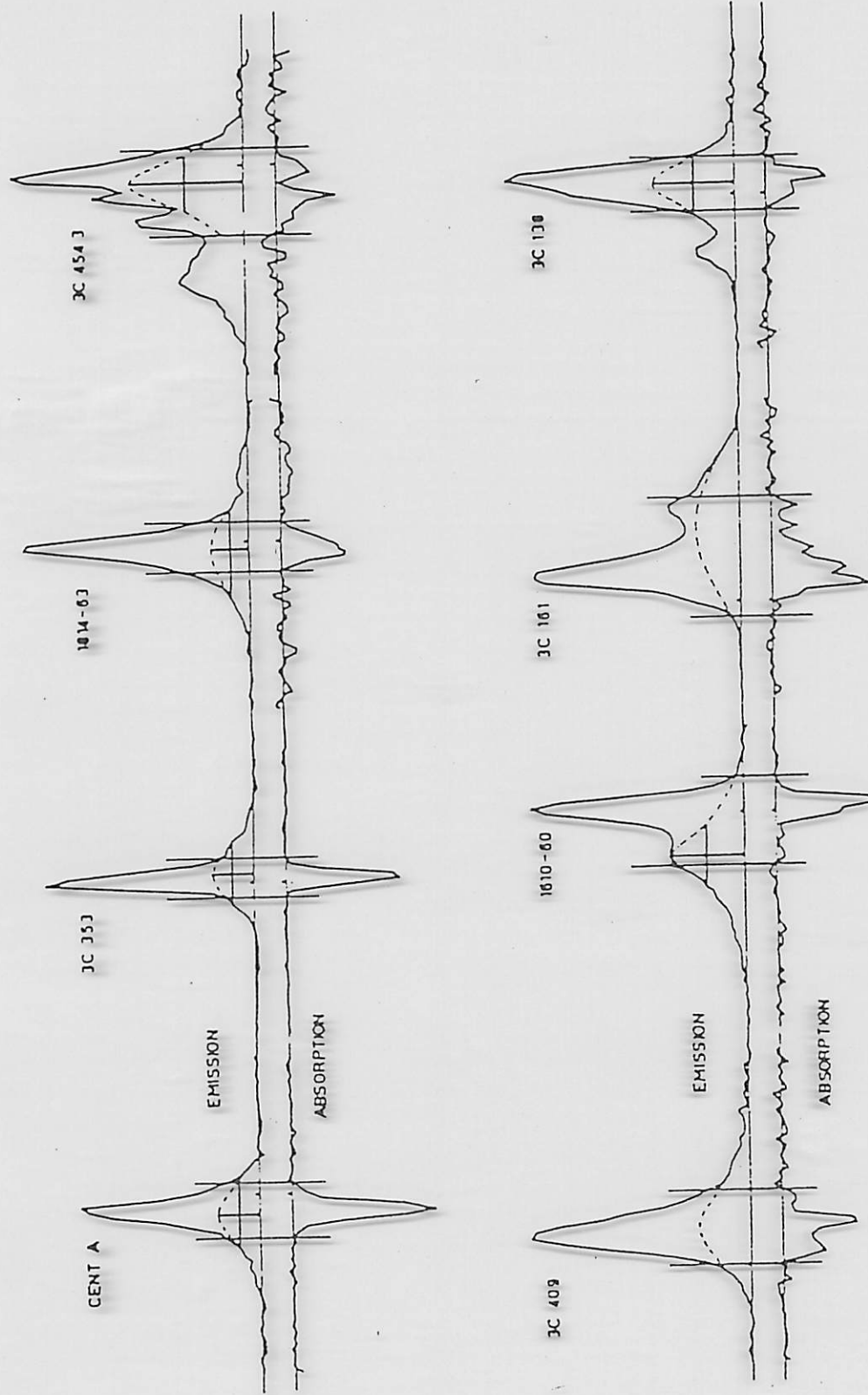


Figure 4-1. A set of high latitude emission and absorption spectra from the Parkes survey (Radhakrishnan et al. 1972).

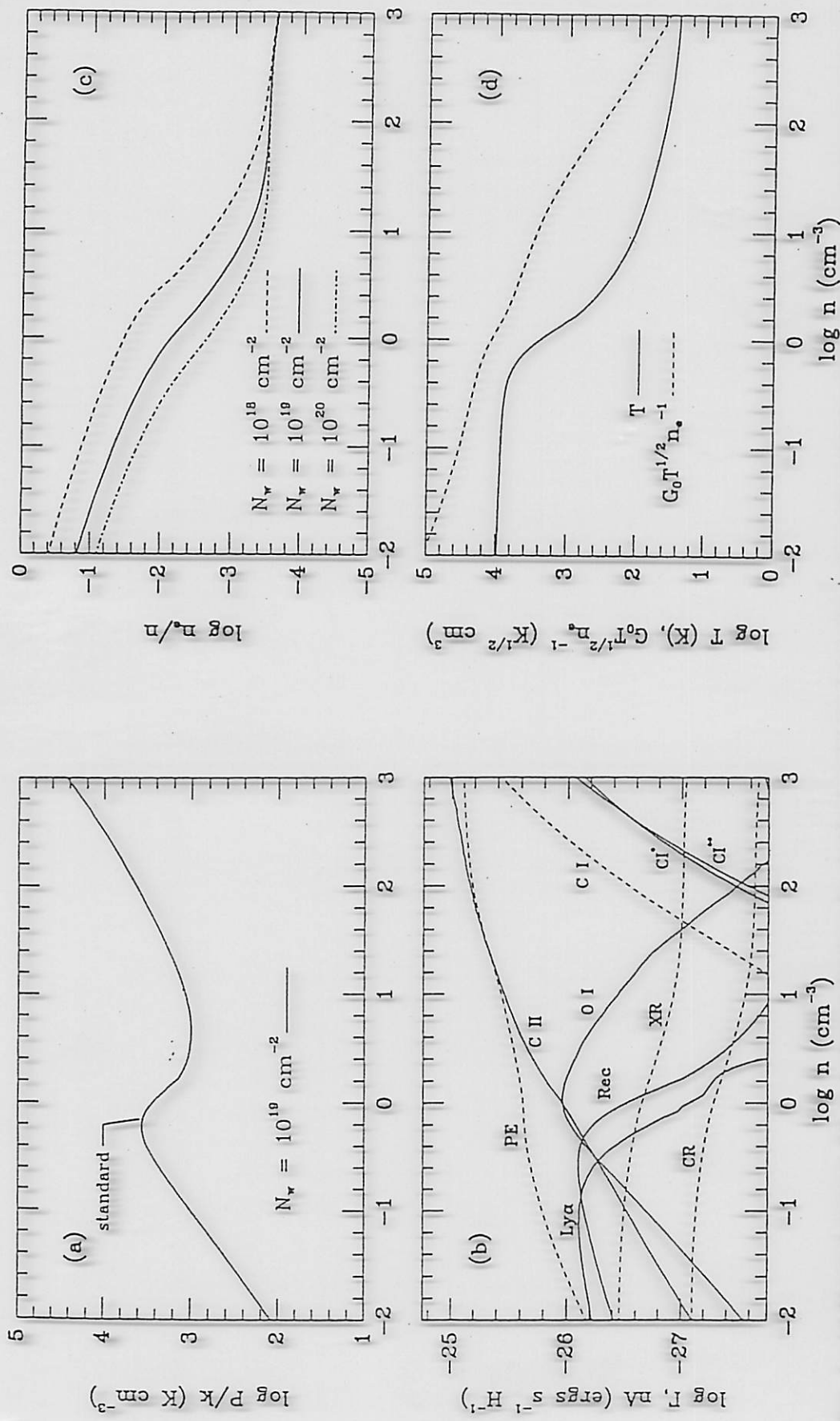


FIG. 3.—(a) Thermal pressure P/k vs. hydrogen density n for standard model (see § 3.1). Gas is thermally stable for $d(\log P)/d(\log n) > 0$. (b) Heating and cooling rates per hydrogen nucleus vs. density n for pressure curve of panel a. Heating rates (dash); Photoelectric heating from small grains and PAHs (PE); X-ray (XR); Cosmic ray (CR); photoionization of C(C I). Cooling rates (solid); C II fine-structure (C II); O I fine-structure (O I); Recombination onto small grains and PAHs (Rec); Ly α plus metastable transitions (Ly α); C I fine-structure 370 μm (C I 1*); C I fine-structure 609 μm (C I 1*). (c) Electron fraction n_e/n as a function of hydrogen density n for the pressure curve of panel a (solid). Also shown are curves for $N_w = 10^{18} \text{ cm}^{-2}$ (dash), and $N_w = 10^{20} \text{ cm}^{-2}$ (dashed), and $N_w = 10^{19} \text{ cm}^{-2}$ (dash-dot). (d) Gas temperature T (solid) and ionization parameter $G_0 T^{1/2} n_e$ (dash) as a function of hydrogen density n for the pressure curve of panel a.